

## Fluctuations in the spectra of open few-body systems

Johannes Eiglsperger<sup>1,2,3</sup>, Tobias Kramer<sup>1,3</sup> and Javier Madroño<sup>2,3</sup>

<sup>1</sup> Institut für Theoretische Physik, Universität Regensburg, D-93040 Regensburg, Germany

<sup>2</sup> Physik Department, Technische Universität München, D-85747 Garching, Germany

E-mail: [johannes.eiglsperger@physik.uni-regensburg.de](mailto:johannes.eiglsperger@physik.uni-regensburg.de), [tobias.kramer@physik.uni-regensburg.de](mailto:tobias.kramer@physik.uni-regensburg.de) and [jmadrone@ph.tum.de](mailto:jmadrone@ph.tum.de)

*New Journal of Physics* **13** (2011) 063033 (15pp)

Received 10 December 2010

Published 17 June 2011

Online at <http://www.njp.org/>

doi:10.1088/1367-2630/13/6/063033

**Abstract.** We investigate simple open few-body systems, the spectra of which exhibit fluctuating patterns, and review the conditions for the existence of an Ericson regime in deterministic, open quantum systems. A widely used criterion, the Lorentzian shape of the autocorrelation function of the spectrum, is shown to be insufficient for the occurrence of Ericson fluctuations: integrable systems or open systems that are not in the Ericson regime might display such an autocorrelation function. We also investigate the sensitivity of Ericson fluctuations on simplified models of realistic systems. In particular, we show that a simplified hydrogenic model for alkali atoms in crossed magnetic and electric fields does not yield Ericson fluctuations for a choice of the energy and field parameters where the realistic system is in the Ericson regime.

<sup>3</sup> Authors to whom any correspondence should be addressed.

**Contents**

<b>1. Introduction</b>	<b>2</b>
<b>2. Conditions for Ericson fluctuations</b>	<b>4</b>
<b>3. Spectral fluctuations and the transition from classically integrable to chaotic systems</b>	<b>4</b>
<b>4. Photoionization cross-sections of planar helium</b>	<b>7</b>
<b>5. Rydberg atoms in crossed electromagnetic fields</b>	<b>11</b>
<b>6. Conclusions</b>	<b>12</b>
<b>Acknowledgments</b>	<b>14</b>
<b>References</b>	<b>14</b>

**1. Introduction**

The experimental characterization and theoretical understanding of complex quantum transport phenomena is of fundamental relevance for many research areas that exploit quantum interference effects for the purpose of an ever-improving control over the quantum dynamics of increasingly complicated systems [1–8]. The origin of the complex quantum dynamics in this context is diverse: deterministic chaos, disorder or many-particle interactions. In any case, an enhanced sensitivity to small changes in some control parameter enforces a statistical description such as to isolate robust quantities to characterize the underlying physical processes. Surprisingly, many of the resulting predictions are universal in character; that is, they apply to, at first glance, rather different classes of physical objects, which only share an increased density of states, and the nonperturbative coupling of their various degrees of freedom.

Erratic fluctuations in some experimental observable under changes in a control parameter are not really surprising in many-particle dynamics or in disordered systems [1, 4, 9–11]. However, they remain rather counterintuitive and, in some cases, are not completely understood in simple quantum systems with only a few degrees of freedom. For example, in single-particle dynamics, classical chaos arises due to a combination of the Coulomb force and a uniform magnetic field. Despite their different origins it is expected that the fluctuations exhibit very similar statistical behavior. For a quantum system with a well-defined classical analogue, the appearance of Ericson fluctuations is commonly accepted as a signature of chaotic scattering [12] and has been recently identified with chaotic transport through cavities [13]. They manifest as random fluctuations in the excitation cross-sections in the regime of highly excited resonance states, with typical decay widths larger than the average level spacing, such that single maxima in the cross-section can no longer be identified with single resonances. Rather they are due to the interference of several of them. These fluctuations were predicted by Ericson in the 1960s [14, 15] in compound nuclear reactions using a simple statistical model for the nuclear scattering matrix. Ericson's proposal translated into an important boost to nuclear reaction studies and since then several realizations of Ericson fluctuations have been found in nuclear physics (see e.g. [16] for a review). Despite the stochastic nature of Ericson fluctuations, the connection between Ericson's model and random matrix theory (RMT) remained an open question for some years. Now Ericson fluctuations are well

understood in nuclear collisions (see e.g. [16, 17]). A widely used fingerprint of Ericson fluctuations is the Lorentzian decay of the spectral autocorrelation function. Ericson [14] showed that a spectrum of overlapping resonances with Lorentzian or Fano profiles leads to a Lorentzian shape of the autocorrelation function, where the width of this function is the mean width of the resonances. Starting with [18], autocorrelation functions and other properties of scattering matrix elements and cross-sections have been investigated in a number of microwave-cavity experiments, for example [11, 18–20]. The theoretical treatment of these systems is usually based on RMT. Among other issues, cross-sections and correlation functions for integrable and chaotic systems have been thoroughly investigated [21, 22] and studies of the circumstances under which the Ericson regime is reached [23] have been conducted in this framework.

After the discovery of Ericson fluctuations, there was speculation for a long time regarding their universal character and about the existence of an Ericson regime in open deterministic quantum systems. Natural candidates for the existence of Ericson fluctuations in atomic systems are highly doubly excited states of helium and ions or atoms in external electric and magnetic fields. So far, the only deterministic open systems where strong evidence for the existence of an Ericson regime has been found are hydrogen and Rydberg alkali atoms interacting with crossed electric and magnetic fields [24–26]. For helium, the existence of Ericson fluctuations still awaits full experimental and theoretical confirmation, despite the significant effort invested in that direction [27–33]. Simplified approaches had, however, predicted the existence of an Ericson regime in helium. One-dimensional (1D) models predict the Ericson regime starting around the 34th single ionization threshold of helium [27, 29]. Xu *et al* [31] have claimed that Ericson fluctuations occur in the inelastic electron impact excitation cross-sections of  $\text{He}^+$  above the 15th single ionization threshold. For that purpose they have used the  $s^2$ -model of helium and the autocorrelation function as the only criterion for the existence of Ericson fluctuations.

In this paper, we show that the spectral information alone does not allow one to determine the chaotic or integrable nature of atomic systems. We discuss the occurrence of (i) Ericson-like fluctuations in classically integrable systems and we also point out that (ii) the description of Ericson fluctuations requires the consideration of all relevant degrees of freedom (and internal structures). Simplified models might lead to wrong conclusions. Also, (iii) the statistical analysis of the spectrum is not sufficient for the description of Ericson fluctuations. For instance, the absence or presence of a Lorentzian shape of the autocorrelation function of a spectrum is not a sufficient condition for determining whether the underlying classical system shows regular or irregular dynamics. For that purpose, after reviewing the conditions necessary for the occurrence of Ericson fluctuations in section 2, we consider three different systems that exhibit fluctuating cross-sections. In section 3, we show that a Lorentzian autocorrelation function in the photodetachment and photoionization of hydrogenic atoms in external fields occurs independently of whether the underlying classical dynamics is chaotic or integrable. The regime of highly excited states of planar helium up to the 20th single ionization threshold is discussed in section 4. We show that the autocorrelation function of the photoionization cross-section again has a Lorentzian shape, despite the fact that the Ericson regime is not reached. Section 5 is devoted to hydrogen and Rydberg alkali atoms in crossed electric and magnetic fields. Each of these systems exhibits Ericson fluctuations. However, the onset of the Ericson regime in these systems does not coincide, which further implies that Rydberg alkali atoms cannot be modeled by the simplified hydrogen atom.

## 2. Conditions for Ericson fluctuations

The Ericson regime in chaotic scattering is completely characterized by strong overlapping of the resonances; that is, the mean width  $\bar{\Gamma}$  of the resonances must be much larger than the mean level spacing  $\bar{s}$ ,  $\bar{\Gamma}/\bar{s} \gg 1$ . A consequence of the chaoticity of the system is that the weights of the resonances are comparable, as expected from RMT [34]. The cross-section can be given as a sum over resonances described by complex-valued poles,

$$\sigma(E) = \text{Im} \left[ \sum_i \frac{A_i}{E - E_i} \right], \quad (1)$$

where  $E_i$  denotes the complex valued resonances in the lower complex energy plane (with  $\text{Im}(E) < 0$ ) and  $A_i$  are the weights of the poles. In the Ericson regime, the cross-section exhibits a random-like fluctuating pattern. In such a case Ericson [14] showed that the autocorrelation function

$$C(\Delta E) = \int_{E_1}^{E_2} dE \sigma(E) \sigma(E + \Delta E) \quad (2)$$

yields a Lorentzian decay with a width equal to the mean width  $\bar{\Gamma}$  of the resonances,

$$C(\Delta E) \sim \frac{1}{1 + (\Delta E/\bar{\Gamma})^2}. \quad (3)$$

The description of a spectrum in the continuum in terms of resonances is well established for Hamiltonians involving the Coulomb potential and, in addition, external electric and magnetic fields. The method of complex scaling [35–39] allows one to directly calculate the position of resonances and to construct the spectrum from this information. Thus, a complex scaling calculation does directly provide information about the statistics of the poles and their spacing. This information is crucial to verify whether the conditions given above are fulfilled. In an experiment, it is not possible to measure the location of the complex poles. Rather, one obtains the cross-sections at real valued energies and also one obtains the autocorrelation function directly from the cross-sections. However, the autocorrelation function alone is not a sufficient condition for Ericson fluctuations, as we will see in the following sections.

## 3. Spectral fluctuations and the transition from classically integrable to chaotic systems

In photoionization and photodetachment experiments, the cross-section of released electrons has been measured with astonishing precision [24, 40]. The high precision is reached by placing the atom or ion in a region where an electric or magnetic field is present, which guides the electron after the detachment from the atom or residual ion to the detector [41, 42]. The basic Hamiltonian for photoionization and photodetachment of hydrogenic atoms in homogeneous perpendicular electric and magnetic fields is given by

$$H = \frac{\mathbf{p}^2}{2} - \frac{Z}{r} + \frac{1}{2} B \ell_z + \frac{1}{8} B^2 (x^2 + y^2) + Fx, \quad (4)$$

where  $B$  denotes the magnetic field, and  $F$  the electric field,  $\ell_z$  the angular momentum projection on the magnetic field axis and  $Z$  the charge of the remaining atom or ion after the electron is ejected due to the absorption of a photon. For atoms or ions with more than

one electron, we neglect the internal structure, which is still a good approximation near threshold [43]. The Hamiltonian equation (4) has a rich spectral structure, depending on the values of  $B$ ,  $F$  and  $Z$ . It yields an integrable dynamics either in the absence of the Coulomb term ( $Z = 0$ ) or alternatively in the absence of the magnetic field ( $B = 0$ ). If  $Z$  and  $B$  are present, the dynamics is chaotic. A universal Lorentzian behavior emerges for the autocorrelation function of the spectra, independent of the chaotic or integrable nature of the underlying dynamics. This observation is important for answering the question of whether a Lorentzian autocorrelation function is caused by irregular scattering, or rather indicates a universal behavior in the presence of external fields (as proposed in [44]). Distinguishing between these two scenarios is a serious experimental problem, since the strict validation of the Ericson condition in terms of complex poles requires us to determine these poles, which cannot be achieved experimentally for overlapping resonances. Note that we discuss in the following merely the class of Hamiltonians contained in equation (4), and we are not constructing an artificial replacement Hamiltonian emulating spectral features, but describing completely different physical processes.

In the following, we discuss the origin of spectral fluctuations in equation (4) in terms of semiclassical closed-orbit theory, taking into account bifurcations and catastrophe theory [45–47]. For the case  $Z = 1$ ,  $F \gg 0$  and  $B = 0$  (classically integrable case), the photoionization spectrum shows fluctuations and a Lorentzian autocorrelation function [44] (figure 7(a)). A detailed semiclassical analysis of the Hamiltonian shows that ionization trajectories can be trapped for extremely long times in the vicinity of the nucleus and that the cross-section is caused by interference of an infinite number of trajectories [48]. Similar observations of long-trapped orbits have been reported for the case  $Z = 1$ ,  $B \gg 0$  and  $F \gg 0$ , suggesting similarities between the integrable and chaotic systems. Another illuminating example is the second integrable case ( $Z = 0$ ,  $B \gg 0$ ,  $F \gg 0$ ) describing photodetachment in crossed electric and magnetic fields. This system has been probed by photodetachment experiments [49, 50] and the measurements agree very well with the theoretical calculation based on the source approach [43, 50] and can be analyzed in closed-orbit theory [51]. The spectral fluctuations originate again from the interference of many orbits and result in a Lorentzian autocorrelation function. We demonstrate some basic features of the cross-section, which are already present in the 2D version of equation (4) with  $p_z$  being absent and  $Z = 0$ . The local density of states (LDOS) is known in closed form [52] and the cross-section for s-wave photodetachment is directly proportional to the LDOS [43]. The LDOS consists of a sequence of Landau levels centered around the energies  $E_n = \hbar\omega_c(n + \frac{1}{2})$  with quantum number  $n$ . The Landau levels are broadened by the electric field such that each Landau level has modulations with  $n$  zeros located at energies  $E_{n,k}$ , where  $k = 0, \dots, n - 1$ . The overall width of a Landau level can be estimated from the classical turning points of a harmonic oscillator to be  $W_n = Fl_B\sqrt{2n+1}$ , where  $l_B = \sqrt{\hbar/(eB)}$  denotes the magnetic length. The mean spacing of the modulations and their width is given approximately by  $W_n/n = Fl_B\sqrt{2n+1}/n$ . Adjacent Landau levels will start to overlap when the level width  $W_n$  exceeds the spacing between their centers:  $W_n > \hbar\omega_c$ . Then, at a given energy, structures in the LDOS arise from a superposition of modulations from several Landau levels  $E_{n,k}$ . This situation can be thought of as an overlap of the sidebands ( $n, k$ ) from different major quantum numbers  $n$ .

Figure 1(a) displays the oscillatory structure of a single Landau level in the presence of an electric field. In figure 1(b), the neighboring Landau levels are included and the cross-section attains a complicated modulation due to the overlapping domains of each Landau level.

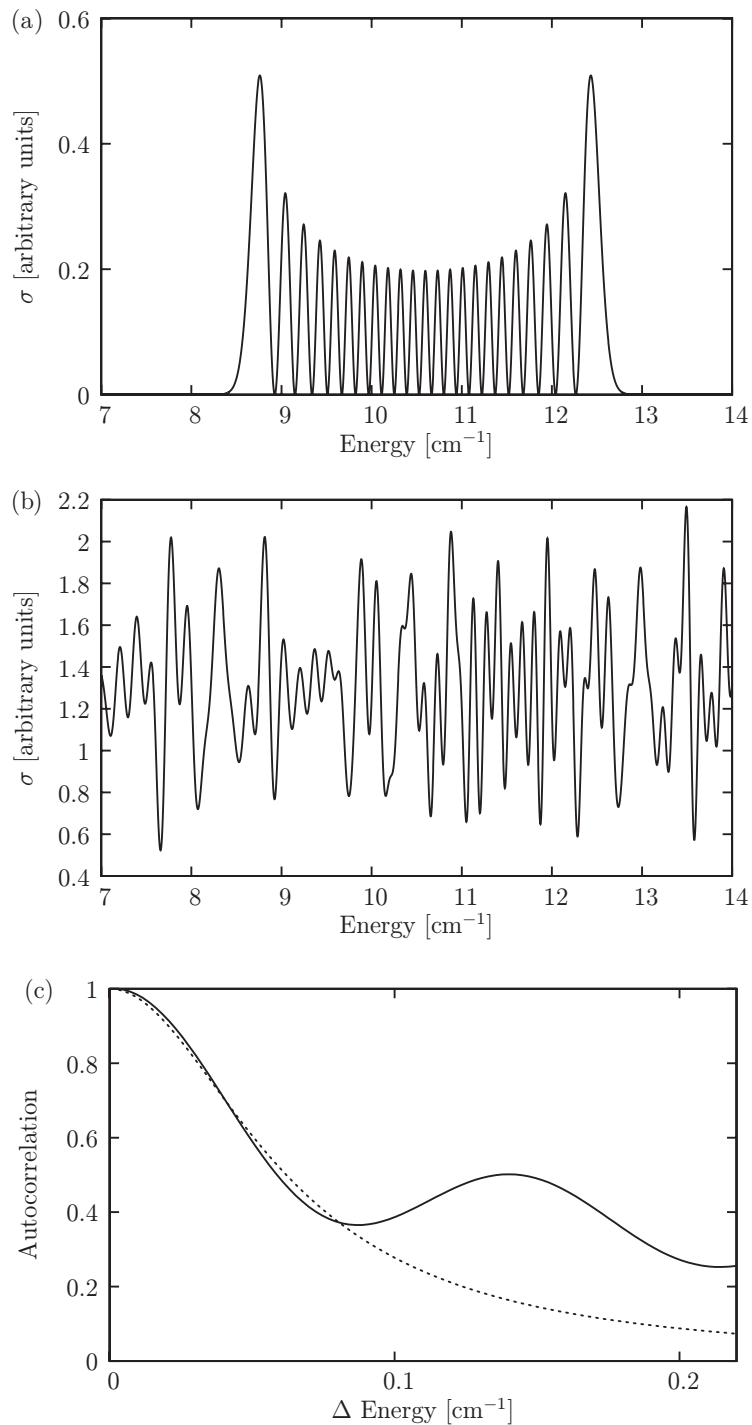


**Figure 1.** Cross-section and autocorrelation of the 2D photodetachment model in perpendicular electric ( $F = 1 \text{ kV m}^{-1}$ ) and magnetic fields ( $B = 0.5 \text{ T}$ ). The Landau level  $n = 22$  is shown in (a). The cross-section (b) results from many overlapping Landau levels, each centered at  $E_n = \hbar\omega_c(n + \frac{1}{2})$ . The autocorrelation function (solid line in panel (c)) attains a Lorentzian shape (dashed line) for  $\Delta < 0.1 \text{ cm}^{-1}$ .

The resulting autocorrelation function of the cross-section approaches a Lorentzian shape for  $\Delta E < 0.1 \text{ cm}^{-1}$  (figure 1(c)) and also displays strong revivals at larger values of  $\Delta E$ . Similar revival effects can be seen in the photoionization cross-sections for classically chaotic systems (see [44] and figure 4 of [53]). While the 2D system has only model character, the 3D calculation for negative ions in a magnetic field leads to Zeeman splittings with additional energy shifts and thus we obtain an even earlier onset of the overlap of neighboring Landau levels [50]. Calculations in parallel electric and magnetic fields show a similar behavior, since the cross-section is fluctuating due to an intricate interference structure of closed orbits [47]. We conclude that a Lorentzian autocorrelation function seems to be a generic feature of equation (4) and thus is not necessarily related to chaotic scattering.

#### 4. Photoionization cross-sections of planar helium

The helium atom is, due to its dramatically increasing density of states near the total breakup threshold another candidate for the existence of Ericson fluctuations in an atomic system. The regime of strongly overlapping resonances, often called the Ericson regime, is reached around the ninth threshold. However, neither experimental nor theoretical photoionization cross-sections up to  $I_{17}$  [30] show signs of Ericson fluctuations. The absence of Ericson fluctuations can be ascribed to a hierarchy of contributions to the cross-section, which leads to a dominant series of resonances associated with an approximate quantum number  $F = N - K^4$ , where  $N$  and  $K$  are approximate quantum numbers from Herrick's algebraic classification [55, 56]. Furthermore, it is shown that the dominant contributions are due to resonances associated with almost collinear configurations and that, under the constraint that the picture of one dominant series is valid, the existence of Ericson fluctuations is expected, as for 1D helium, around  $I_{34}$  [30].

For planar helium [32, 57–59], a model system with reduced complexity that nevertheless gives a good qualitative and even quantitative description [58, 60], the existence of a dominant series associated with an approximate quantum number  $F$  has been verified up to  $I_{20}$  [32, 33]. Moreover, apart from the dominant contribution, further minor contributions to the fluctuations in the photoionization cross-section have been analyzed and an apparent breakdown of the picture of one dominant series of resonances, which would lead to an earlier onset of Ericson fluctuations, has been observed.

The Hamiltonian describing the unperturbed helium atom, in atomic units, and assuming an infinite mass of the nucleus, reads

$$H = \frac{\vec{p}_1^2 + \vec{p}_2^2}{2} - \frac{2}{r_1} - \frac{2}{r_2} + \frac{1}{r_{12}}. \quad (5)$$

Here,  $\vec{p}_1$ ,  $\vec{p}_2$  and  $\vec{r}_1$ ,  $\vec{r}_2$  are the momenta and positions of electron one and two, respectively, whereas  $r_{12}$  is the interelectronic distance. In planar helium, the dynamics are confined to a 2D configuration space. The choice of appropriate coordinates leads to a representation in terms of four creation and annihilation operators  $a_j, a_j^\dagger$ ,  $j = 1, 2, 3, 4$  [57, 61]. In combination with the complex rotation method [35–39], the diagonalization of the associated generalized eigenvalue problem provides complex eigenvalues  $E_{i,\theta}$ —which includes resonances and continuum states—and the corresponding eigenvectors  $|\psi_{i,\theta}\rangle$ . Resonances of the system are independent

<sup>4</sup> A similar approximate quantum number  $v = N - K - 1$  has been introduced in [54] and is connected to harmonic bending vibrations of the linear  $eZe$  configuration.

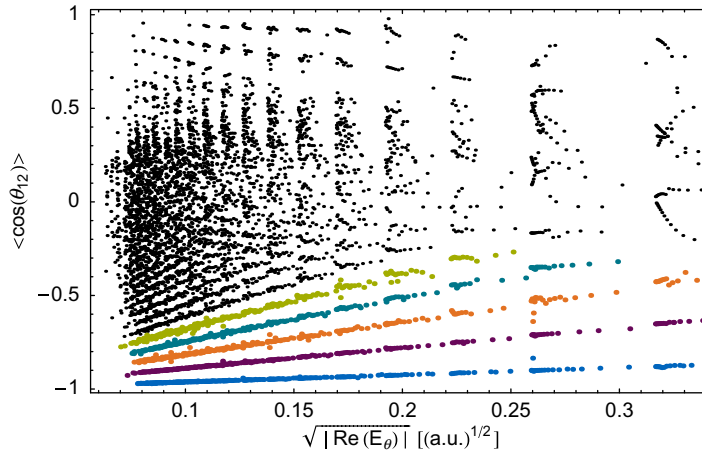


**Figure 2.** Calculated  $\langle \cos(\theta_{12}) \rangle$  values as a function of resonance energy  $E$  below the 20th threshold for triplet planar helium. The region  $|\langle \cos(\theta_{12}) \rangle| < 0.5$  also includes some converged resonances up to below  $I_{23}$ . Each point represents a particular triplet state resonance with  $\Pi_x = +1$  and  $|l| = 1$ . The resonances are displayed in color according to their allocation to Rydberg series: ● (1st), ● (2nd), ● (3rd), ● (4th), ● (5th) and ● for resonances not identified with any of these series. Reproduced from [32] with permission. Copyright 2009 by the American Physical Society.

of the complex rotation angle  $\theta$ , and their energies  $E_i$  and widths  $\Gamma_i$  are contained within the corresponding eigenvalue:  $E_{i,\theta} = E_i + i\Gamma_i/2$ . Within the framework of the complex rotation method, total photoionization cross-sections (1) take the form

$$\sigma(\omega) = \frac{4\pi\omega}{c} \text{Im} \left[ \sum_i \frac{\langle \psi_{i,\theta} | R(\theta) T | \phi_E^{\text{in}} \rangle^2}{E_{i,\theta} - E_{\text{in}} - \omega} \right], \quad (6)$$

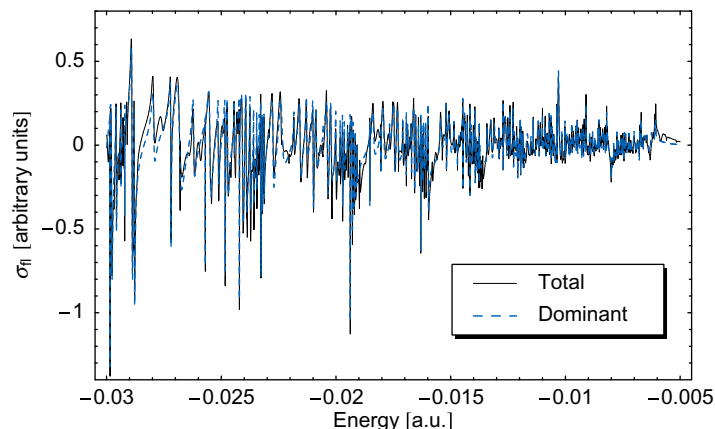
with  $\omega$  being the energy of the photon,  $T$  the dipole operator,  $R(\theta)$  an operator of the complex rotation method and  $|\phi_E^{\text{in}}\rangle$  the initial state with energy  $E_{\text{in}}$ . For the computation of the fluctuations in the cross-section, differing only by a smooth background from the actual cross-section, only resonance states are used as final states in (6) [32, 33].

Figure 2 presents a plot of the calculated expectation values  $\langle \cos(\theta_{12}) \rangle$  as a function of  $\sqrt{|\text{Re}(E_\theta)|}$  for all converged resonances from  $I_4$  up to  $I_{23}$ .<sup>5</sup>  $\theta_{12}$  is the angle between the two electron position vectors  $\vec{r}_1$  and  $\vec{r}_2$ . A clear decomposition into series of resonances can be identified for  $\langle \cos(\theta_{12}) \rangle \lesssim -0.5$ . From the relation

$$\langle \cos(\theta_{12}) \rangle \xrightarrow{n \rightarrow \infty} -\frac{K}{N}, \quad (7)$$

the  $eZe$  configuration can be identified with the maximum value of  $K = N - 1$ , i.e.  $F = N - K = 1$ . Furthermore, the values of  $\langle \cos(\theta_{12}) \rangle$  in the low-lying series in figure 2 decrease smoothly with decreasing values of  $\sqrt{|\text{Re}(E_\theta)|}$ . The approximate quantum number  $F = N - K$  thus allows the classification of these series of resonances, all members of which lie on straight lines. As the energy approaches the total fragmentation threshold, new series associated with higher values of  $F$  appear. Extrapolations of the straight lines for series

<sup>5</sup> A detailed description of the computation of  $\langle \cos(\theta_{12}) \rangle$  in the complex rotation method can be found in [62].



**Figure 3.** Comparison of the fluctuations in the photoionization cross-sections from  $I_9$  to  $I_{20}$  including all resonances (solid line) and those resonances with  $F = 1$  only (dashed line). Reproduced from [32] with permission. Copyright 2009 by the American Physical Society.

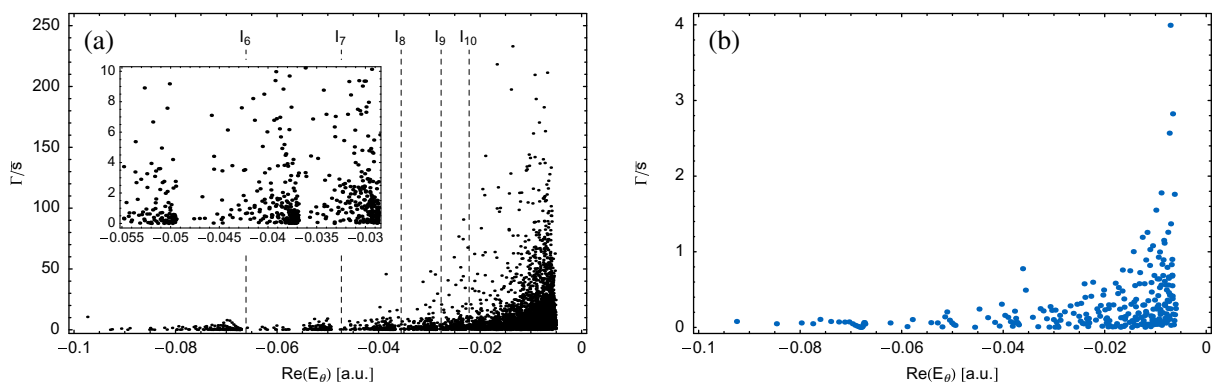


**Figure 4.** Resonance widths in units of the mean level spacing  $\bar{s}$ . Panel (a) shows the widths of all resonance states found in this energy regime, with the inset giving a close-up of the regime around  $I_7$  to  $I_9$ , while panel (b) includes exclusively resonances characterized by  $F = 1$ . The details can be found in [32, 33]. Reproduced from [32] with permission. Copyright 2009 by the American Physical Society.

classified by a constant value of  $F$  cross each other at a value of  $\langle \cos(\theta_{12}) \rangle = -1$  at the double ionization threshold. In this limit, these resonances correspond to the  $eZe$  configuration, which is stable under angular perturbations, but unstable under radial perturbations. Therefore, the existence of the approximate quantum number  $F$  can be understood from the regularity in the angular direction in helium, although the radial motion remains chaotic.

The approximate classification of helium resonances unveiled in figure 2 allows us to study separately the contribution of a subset of resonances to the photoionization cross-section. Indeed, only a small fraction of states contribute significantly to the cross-section, which is also reflected in propensity rules [63]. For triplet planar helium the series associated with  $F = 1$  yields the dominant contribution, which is depicted together with the fluctuations in the photoionization cross-sections including all resonances in figure 3. In figure 4, the widths

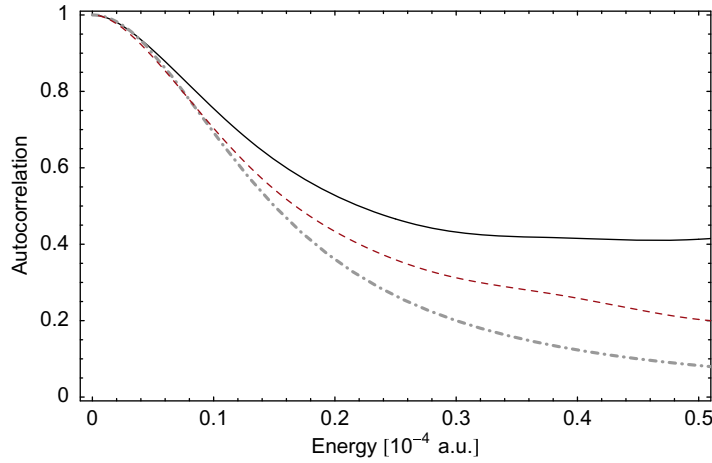


**Figure 5.** Autocorrelation functions of the fluctuations of the cross-section for the energy regime between  $I_{15}$  and  $I_{18}$ . The solid line gives the autocorrelation function including all resonances, while the dashed line is the autocorrelation function for the contribution of the dominant series. In addition, a Lorentz curve of width  $0.15 \times 10^{-4}$  a.u. (dashed-dotted line) is presented that is, up to  $\epsilon \approx 0.1 \times 10^{-4}$  a.u., a good approximation for the autocorrelation function of the dominant series.

of resonances are displayed in units of the local mean level spacing  $\bar{s}$  for all resonances and for members of the resonance series with  $F = 1$  only. It is obvious that including all resonances, the regime of strongly overlapping resonances is reached far below the 10th threshold. The situation changes completely if one considers only the resonances of the dominant series, where the resonances just start to overlap around the 20th threshold.

The autocorrelation functions, equation (2), of the fluctuations in the photoionization cross-section for energy regimes between  $I_{15}$  and  $I_{18}$  show initial Lorentzian form if one considers exclusively the dominant contribution as well as all contributions (figure 5). For larger values of  $\epsilon$ , the autocorrelation functions start to deviate from the Lorentzian shape, which is probably a consequence of the restricted energy regime and the finite number of resolved resonances close to the single ionization thresholds. The widths of both the autocorrelation functions are roughly given by

$$\bar{\Gamma}_{\text{autocorr}} \approx 0.2 \times 10^{-4} \text{ a.u.} \quad (8)$$

However, the computation of the mean width from the widths of the resonances in this energy regime yields two highly different values for considering all resonances and considering exclusively resonances of the dominant series. In the case of the dominant series, the mean width is given by

$$\bar{\Gamma}_{F=1} \approx 0.13 \times 10^{-5} \text{ a.u.}, \quad (9)$$

while the mean width for all resonances is computed to be

$$\bar{\Gamma}_{\text{tot}} \approx 0.36 \times 10^{-4} \text{ a.u.} \quad (10)$$

Apart from these issues, the concept of mean width may be questionable in systems with a spectrum consisting of Rydberg-like series with different accumulation points. This is because a mean width in that case will always be resolution dependent (for both the experiment and theory).

Therefore, although there is apparent agreement with the predictions of Ericson [14], namely that the autocorrelation function takes the form of the Lorentzian shape (3), the evidence presented above shows that the nature of the fluctuations exhibited by the spectrum of planar helium up to the 20th ionization threshold does not correspond to Ericson fluctuations. Once more, as in the situation described in section 3, the autocorrelation function alone might lead to erroneous conclusions.

## 5. Rydberg atoms in crossed electromagnetic fields

In contrast to the situations considered in sections 3 and 4, Rydberg atoms exposed to crossed electric and magnetic fields exhibit Ericson fluctuations [25, 26]. The transition to the Ericson regime has been observed in the photoionization cross-section of rubidium Rydberg states in the presence of crossed fields [24].

The Hamiltonian describing the single-electron Rydberg dynamics subjected to crossed electric and magnetic fields, in atomic units, and assuming an infinite mass of the nucleus reads

$$H = \frac{\mathbf{p}^2}{2} + V_{\text{atom}}(r) + \frac{1}{2}B\ell_z + \frac{1}{8}B^2(x^2 + y^2) + Fx, \quad (11)$$

which is the Hamiltonian (4) where  $-Z/r$  has been substituted by  $V_{\text{atom}}(r)$ . In the case of hydrogenic atoms, the electron–nucleus interaction  $V_{\text{atom}}(r)$  is given by the Coulomb potential. For alkali Rydberg atoms, however, due to the multiparticle nature of the core, no uniquely defined one-particle potential is available.  $V_{\text{atom}}$  is therefore not given explicitly. Nevertheless, the deviation of  $V_{\text{atom}}$  from a strictly Coulombic potential in a small but finite volume around the nucleus can be accounted for by the phase shift experienced by the Rydberg electron upon scattering off the multielectron core [64, 65]. This phase shift is fixed by the  $\ell$ -dependent quantum defects  $\delta_\ell$  of the unperturbed atom, which are precisely determined by spectroscopic data [66]. The presence of both fields destroys all symmetries of the unperturbed Coulomb problem, resulting in a full 3D problem. The description of the coupling to the continuum induced by the crossed fields is achieved with the help of the complex rotation method. A basis of real Sturmian functions leads to complex symmetric matrix representation of the rotated Hamiltonian. The photoexcitation cross section  $\sigma(E)$  is readily obtained from the quantum spectrum, via equation (6). In this case, the relative oscillator strength  $D_{j;L=2} = \langle \overline{\psi_{i,\theta}} | R(\theta) T | \phi_E^{\text{in}} \rangle$  is calculated for the transition from the initial state  $|\phi_E^{\text{in}}\rangle = |n = 5L = 1M = -1\rangle$  with energy  $E_0 \sim -0.002$  a.u. to the  $L = 2$  manifold, mediated by a single photon linearly polarized along the magnetic field axis (thus selecting the odd parity part of the spectrum).

The experiments in [24] probe the energy range from  $-57.08$  to  $-55.92$   $\text{cm}^{-1}$  (corresponding to principal quantum numbers  $n \simeq 43, \dots, 45$  of the bare rubidium atom), at a fixed electric field strength  $F = 22.4$   $\text{kV m}^{-1}$  and for three different values of the magnetic field,  $B = 0.9974, 1.49$  and  $2.0045$  T. The electric field shifts the effective ionization threshold to  $-91.4$   $\text{cm}^{-1}$  at the Stark saddle; hence, the experimentally probed energy range lies clearly in the continuum part of the spectrum.

A detailed theoretical analysis of the experimental situation shows that the laboratory results indeed entered the regime of overlapping resonances. Approximately 65% of all resonance eigenstates contributing to the photoabsorption signal have widths that are *larger* than the mean-level spacing  $\Delta$  and half of these resonances have a width that is at least 10 times larger than the mean-level spacing. Figure 6 shows the numerically calculated distribution of

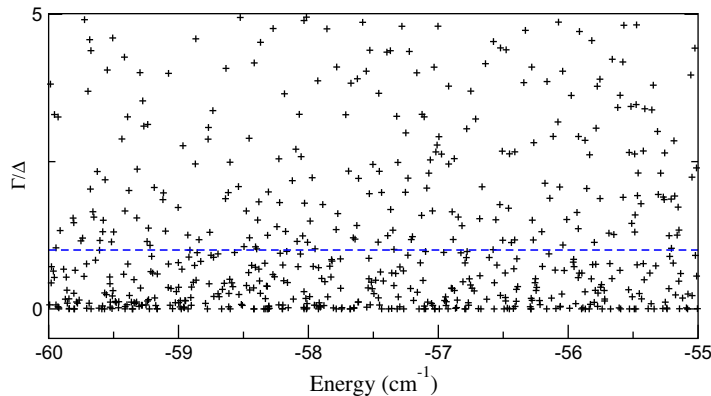


**Figure 6.** Close-up ( $0 \leq \Gamma/\Delta \leq 5$ ) of the distribution of the computed resonance widths  $\Gamma_j$  in an energy interval that covers the experimentally [24] scanned energy region for  $B = 2.0045$  T and  $F = 22.4$  kV m $^{-1}$ . The dashed line indicates the average spacing  $\Delta$  of the resonance states on the energy axis. Not shown are resonances present at  $\Gamma/\Delta \geq 5$ . The majority of all computed resonances lie above  $\Gamma_j > \Delta$ . Adapted from [25] with permission. Copyright 2005 by the American Physical Society.

resonance widths over the energy range probed by the experiment, under precisely equivalent conditions as in the experiment (fixed by the strength of the magnetic and electric fields). The cross sections  $\sigma(E)$  for four values of the magnetic field  $B$  are displayed in figure 7 for rubidium atoms on the left-hand side and for hydrogen on the right-hand side. Due to the scale invariance of the classical dynamics in a Coulomb potential, the specific choice of  $F$  and  $B = 2.0045$  T is equivalent to the one in [53] (there for the purely Coulombic problem, and for a lower-lying energy range,  $n \simeq 19, \dots, 22$ , i.e. at much reduced spectral densities), which corresponds to classically chaotic scattering (where electric and magnetic fields are of comparable strength, although incompatible symmetry). In the case of hydrogen, the cross-section exhibits erratic fluctuations. As the magnitude of the magnetic field decreases, the level of chaoticity diminishes and accordingly the spectrum starts to be dominated by isolated resonances (see the right-hand side of figure 7 and [53]). The scaling invariance mentioned above might be used as an approximate guide into the regime of broken symmetries of the quantum problem for the case of alkali atoms. Indeed, the cross sections of rubidium for  $B = 2.0045$  T exhibit strong fluctuations. However, the finite-size multielectron core of rubidium, strictly speaking, invalidates such a scaling argument [65], as well as a strict quantum-classical analogy, due to the absence of a well-defined classical one-particle analogue. Indeed, in all the cross sections for rubidium atoms shown in figure 7 (left-hand side) many of the structures with a width smaller than  $\bar{\Gamma}$  can no longer be associated with single isolated resonances, and thus indicate the interference of different decay amplitudes.

## 6. Conclusions

We have given examples of atomic systems where the Lorentzian decay of the autocorrelation function is not connected to classical chaotic dynamics, demonstrating that the autocorrelation function of a cross-section does not provide sufficient information to identify Ericson

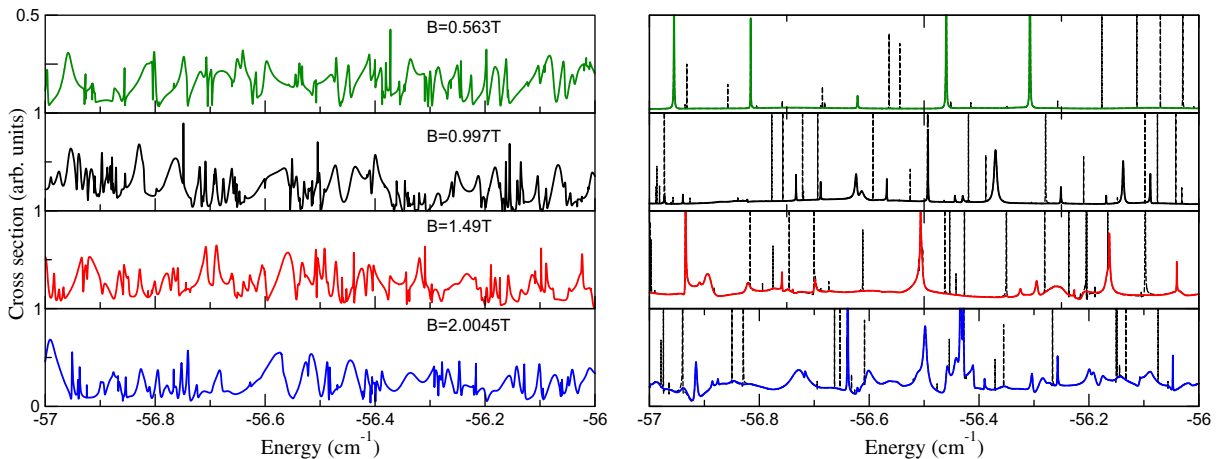


**Figure 7.** Numerically obtained photo cross-section (6) of rubidium Rydberg (left) and hydrogen (right) states in crossed electric and magnetic fields [25] deduced from a parameter-free diagonalization of the Hamiltonian (11), using exactly the experimental parameters [24]  $F = 22.4 \text{ kV m}^{-1}$  and  $B = 2.0045 \text{ T}$ ,  $B = 1.49 \text{ T}$  and  $B = 0.9974 \text{ T}$ . In addition, also the cross-sections for  $B = 0.563 \text{ T}$  and  $F = 22.4 \text{ kV m}^{-1}$  are shown. The spectrum of hydrogen contains in any case very narrow resonances. The dashed lines show the cross-sections obtained by including all resonances of the spectrum. The solid lines on the left-hand side have been obtained by including only those resonances whose half-widths are larger than  $10^{-8} \text{ a.u.}$  ( $\approx 0.0022 \text{ cm}^{-1}$ ). Adapted from [25] with permission. Copyright 2005 by the American Physical Society.

fluctuations. Our observations point to another physical mechanism causing spectral fluctuations, namely the interference of a large number of classical trajectories with differing classical actions. This seems to be a very generic feature of atomic systems exposed to external fields.

Even in classical chaotic systems, Ericson fluctuations can be absent due to the occurrence of dominant series of resonances, which render the definition of a mean resonance width questionable and do not allow us to identify the mean width with the width of the autocorrelation function. Photoionization cross sections in helium are dominated by series of states associated with approximative quantum numbers. Therefore, the observation of Ericson fluctuations in photoionization cross-sections of helium requires the resolution of these dominant series, which cannot be achieved within simplified models such as 1D or  $s^2$  models, as these do not include relevant degrees of freedom.

Ericson fluctuations do occur in Rydberg states of alkali atoms, but require us to take into account the effects of the non-Coulombic core potential. A simplified hydrogenic model does not yield Ericson fluctuations for the same magnetic field parameters.

The unambiguous observation of Ericson fluctuations remains a difficult task and requires a careful consideration of all the relevant degrees of freedom and interference phenomena that affect the cross-section. Interpretation of a Lorentzian decay of an autocorrelation function in terms of a mean-level width is, in general, not possible.

Note that studies of integrable and chaotic time reversal invariant systems on the basis of RMT suggest that cross correlation functions [22] might be a better choice for identifying the occurrence of Ericson fluctuations. However, cross-correlation functions would require the computation of partial cross sections, which is not possible within our complex rotation approach. A recent publication [23] also suggests, based on RMT studies, the use of higher moments of correlation functions in order to identify the exact onset of Ericson fluctuations, which seems to be, given the deviations for large values of  $\epsilon$ , not feasible in atomic physics or in open deterministic many-body systems in general. Nevertheless, these studies also confirm our conclusion that identification of classical chaotic dynamics or Ericson fluctuations solely based on the Lorentzian decay of the autocorrelation function is not possible.

## Acknowledgments

Access to the computing facilities of ‘Leibniz-Rechenzentrum der Bayerischen Akademie der Wissenschaft’, as well as financial support from Deutsche Forschungsgemeinschaft under contract numbers FR 591/16-1 and MA 3305/2-2 and the Emmy-Noether Program (KR 2889/2), is gratefully acknowledged.

## References

- [1] Dittrich T *et al* 1998 *Quantum Transport and Dissipation* (Weinheim: Wiley)
- [2] Buchleitner A, Guarneri I and Zakrzewski J 1998 *Europhys. Lett.* **44** 162
- [3] Müller C and Miniatura C 2002 *J. Phys. A: Math. Gen.* **35** 10163
- [4] Kolovsky A R and Buchleitner A 2003 *Phys. Rev. E* **68** 056213
- [5] Wimberger S, Guarneri I and Fishman S 2003 *Nonlinearity* **16** 1381
- [6] Hornberger K *et al* 2003 *Phys. Rev. Lett.* **90** 160401
- [7] Wellens T, Gremaud B, Delande D and Miniatura C 2004 *Phys. Rev. A* **70** 023817
- [8] Paul T, Richter K and Schlagheck P 2005 *Phys. Rev. Lett.* **94** 20404
- [9] Borgonovi F and Guarneri I 1992 *J. Phys. A: Math. Gen.* **25** 3239
- [10] Beenakker C W J 1997 *Rev. Mod. Phys.* **69** 731
- [11] Dietz B *et al* 2008 *Phys. Rev. E* **78** 055204
- [12] Blümel R and Smilansky U 1988 *Phys. Rev. Lett.* **60** 477
- [13] Müller S, Heusler S, Braun P and Haake F 2007 *New J. Phys.* **9** 12
- [14] Ericson T 1960 *Phys. Rev. Lett.* **5** 430
- [15] Ericson T 1963 *Ann. Phys.* **23** 390
- [16] Guhr T, Müller-Groeling A and Weidenmüller H A 1998 *Phys. Rep.* **299** 189
- [17] Brody T A *et al* 1981 *Rev. Mod. Phys.* **53** 385
- [18] Doron E, Smilansky U and Frenkel A 1990 *Phys. Rev. Lett.* **65** 3072
- [19] Hemmady S *et al* 2006 *Phys. Rev. B* **74** 195326
- [20] Stöckmann H 1999 *Quantum Chaos: an Introduction* (Cambridge: Cambridge University Press)
- [21] Dittes F-M 2000 *Phys. Rep.* **339** 215
- [22] Gorin T and Seligman T H 2002 *Phys. Rev. E* **65** 026214
- [23] Dietz B *et al* 2010 *Phys. Lett. B* **685** 263
- [24] Stania G and Walther H 2005 *Phys. Rev. Lett.* **95** 194101
- [25] Madroñero J and Buchleitner A 2005 *Phys. Rev. Lett.* **95** 263601
- [26] Main J and Wunner G 1992 *Phys. Rev. Lett.* **69** 586
- [27] Blumel R 1996 *Phys. Rev. A* **54** 5420
- [28] Grémaud B and Delande D 1997 *Europhys. Lett.* **40** 363

- [29] Püttner R *et al* 2001 *Phys. Rev. Lett.* **86** 3747
- [30] Jiang Y H *et al* 2008 *Phys. Rev. A* **78** 021401
- [31] Xu J, Le A-T, Morishita T and Lin C D 2008 *Phys. Rev. A* **78** 012701
- [32] Eiglsperger J and Madroñero J 2009 *Phys. Rev. A* **80** 022512
- [33] Eiglsperger J and Madroñero J 2009 *Phys. Rev. A* **80** 033902
- [34] Blümel R and Smilansky U 1990 *Phys. Rev. Lett.* **64** 241
- [35] Aguilar J and Combes J M 1971 *Commun. Math. Phys.* **22** 269
- [36] Balslev E and Combes J M 1971 *Commun. Math. Phys.* **22** 280
- [37] Simon B 1973 *Ann. Math.* **97** 247
- [38] Reinhardt W P 1982 *Annu. Rev. Phys. Chem.* **33** 223
- [39] Ho Y K 1983 *Phys. Rep.* **99** 1
- [40] Andersen T 2004 *Phys. Rep.* **394** 157
- [41] Blondel C, Delsart C and Dulieu F 1996 *Phys. Rev. Lett.* **77** 3755
- [42] Chaibi W *et al* 2010 *Eur. Phys. J. D* **58** 29
- [43] Bracher C *et al* 2005 *Phys. Lett. A* **347** 62
- [44] Karlsson H O and Goscinski O 1995 *Phys. Rev. A* **51** 1154
- [45] Peters A D and Delos J B 1993 *Phys. Rev. A* **47** 3020
- [46] Peters A D and Delos J B 1993 *Phys. Rev. A* **47** 3036
- [47] Bracher C, Kramer T and Delos J 2006 *Phys. Rev. A* **73** 062114
- [48] Bordas C, Lépine F, Nicole C and Vrakking M J J 2003 *Phys. Rev. A* **68** 012709
- [49] Blumberg W A M, Itano W M and Larson D J 1979 *Phys. Rev. A* **19** 139
- [50] Yukich J N, Kramer T and Bracher C 2003 *Phys. Rev. A* **68** 033412
- [51] Kramer T 2004 *Group Theoretical Methods in Physics (Institute of Physics Conference Series Number 185)* ed L E Vicent, K B Wolf and G Pogosyan (Bristol: Institute of Physics) pp 353–8
- [52] Kramer T, Bracher C and Kleber M 2004 *J. Opt. B: Quantum Semiclass. Opt.* **6** 21
- [53] Main J and Wunner G 1994 *Phys. J. B: At. Mol. Opt. Phys.* **27** 2835
- [54] Herrick D R and Kellman M E 1980 *Phys. Rev. A* **21** 418
- [55] Herrick D R and Sinanoğlu O 1975 *Phys. Rev. A* **11** 97
- [56] Sinanoğlu O and Herrick D 1975 *J. Chem. Phys.* **62** 886
- [57] Madroñero J and Buchleitner A 2008 *Phys. Rev. A* **77** 053402
- [58] Eiglsperger J and Madroñero J 2010 *Phys. Rev. A* **82** 033422
- [59] Eiglsperger J and Madroñero J 2009 *High Performance Computing in Science and Engineering, Garching/Munich 2009* ed S Wagner, M Steinmetz, A Bode and M M Müller (Berlin: Springer) pp 627–37
- [60] Madroñero J *et al* 2005 *Europhys. Lett.* **70** 183
- [61] Hilico L *et al* 2002 *Phys. Rev. A* **66** 022101
- [62] Eiglsperger J, Schönwetter M, Piraux B and Madroñero J 2011 *At. Data Nucl. Data Tables* accepted (arXiv:1105.0742v1)
- [63] Rost J M, Schulz K, Domke M and Kaindl G 1997 *J. Phys. B: At. Mol. Opt. Phys.* **30** 4663
- [64] Halley M H, Delande D and Taylor K T 1992 *J. Phys. B: At. Mol. Opt. Phys.* **25** L525
- [65] Krug A and Buchleitner A 2002 *Phys. Rev. A* **66** 053416
- [66] Lorenzen C J and Niemax K 1983 *Phys. Scr.* **27** 300